Iron imaging using SWIFT in a rat model of traumatic brain injury

Lauri Lehto[1], Curtis Corum[2], Djaudat Idiyatullin[2], Asla Pitkänen[1,3], Michael Garwood[2], Olli Gröhn[1], and Alejandra Sierra[1]

[1]Department of Neurobiology, A. I. Virtanen Institute for Molecular Sciences, University of Eastern Finland, Kuopio, Kuopio, Finland, [2]Center for Magnetic Resonance Research and Department of Radiology, University of Minnesota Medical, Minneapolis, Minnesota, United States, [3]Department of Neurology, Kuopio University Hospital, Kuopio, Finland

INTRODUCTION

Intracranial hemorrhage within brain parenchyma is one of the consequences of traumatic brain injury (TBI). Primary damage from bleeding occurs within minutes to hours after the injury as a result of mechanical damage. The blood may trigger secondary events associated with neuronal hyperexcitability, toxic mechanisms, oxidative stress, and inflammation[1]. The accumulation of blood in brain tissue results in deposits of high iron content, which are paramagnetic and detectable by MRI. To study iron deposits from hemorrhages after traumatic brain injury, we utilized SWIFT (sweep imaging with Fourier transformation)[2], which is an almost zero acquisition delay pulse sequence using gapped frequency swept pulses. Even though there is no time for phase accumulation at k=0, as during a gradient echo, phase behavior is still seen in the acquired data[3]. SWIFT has the advantage of not requiring post-processing (ie, high-pass filtering) to remove residual B_0 variation from shim imperfections and large spatial scale susceptibility fields to achieve useful phase images. SWIFT has previously demonstrated its ability to detect calcifications[3], which can be differentiated from the iron deposits by the polarity of the dipole in imaginary SWIFT images.

MATERIALS AND METHODS

Traumatic brain injury was performed by lateral fluid percussion injury in adult Sprague-Dawley rats (10 TBI, 5 Sham). After 5 months, animals were imaged *in vivo*. After perfusion, they were also imaged *ex vivo*. *In vivo* and *ex vivo* imaging was conducted at 9.4 T horizontal and vertical magnets with Varian Direct Drive consoles using 19 mm quadrature volume and quadrature half volume coils, respectively. SWIFT parameters for *ex vivo* imaging were TR = 5 ms, sw = 62.5 kHz, $\alpha = 5°$, FOV = 3.7^3 cm^3, and for *in vivo* imaging TR = 8.2 ms, sw = 31.125 kHz, $\alpha = 5°$ and FOV = 4.5 x 4.5 x 6 cm^3. Matrix size for all images was 256^3. The area of the deposits was estimated from the *ex vivo* magnitude images and correlated with Nissl and Perl´s (iron) stained sections.

RESULTS

All animals with TBI showed bleeds in several brain areas. Surrounding the lesion, white matter tracts exhibited deposits of high iron content, including the corpus callosum, external capsule and fimbria. Bleeds were also located in gray matter, including the hippocampus, parasubiculum, optic nerve layer and superficial gray layer of the superior colliculus and several cortical areas such as the perirhinal cortex, ectorhinal cortex and temporal association cortex. **Figure 1** shows a representative case imaged *ex vivo* (**Fig. 1A-C**) and *in vivo* (**Fig. 1D**). At the level shown in the images, iron deposits are in the parasubiculum, hippocampus and temporal association cortex. A thalamic calcification can be seems also at this level (black arrowhead in **Fig. 1C**). **Figure 2** shows yellow-brown deposits as revealed by Nissl staining (**Fig. 2A**), and intense blue via Perl´s staining (**Fig. 2B**). The signal detected in SWIFT corresponded to several deposits close to each other in the same location. The number of deposits per area varied between cases. **Figure 3** shows the correlations of two examples of brain areas between MRI and histology. In the hippocampus (**Fig. 3A**), deposits were mostly found in the pyramidal cell layer of CA3, hilus, and infrapyramidal blade of the dentate gyrus including the subgranular zone, granule cell layer and molecular layer. The area of deposits in hippocampal slices ranged from 11.4 to 1719.2 μm^2. All the bleed areas found and matched in the same location as in the *ex vivo* SWIFT images (r=0.50) were pooled. In the optic nerve layer of the superior colliculus (**Fig. 3B**), the areas of the deposits ranged from 4.6 to 468.0 μm^2 (r=0.66).

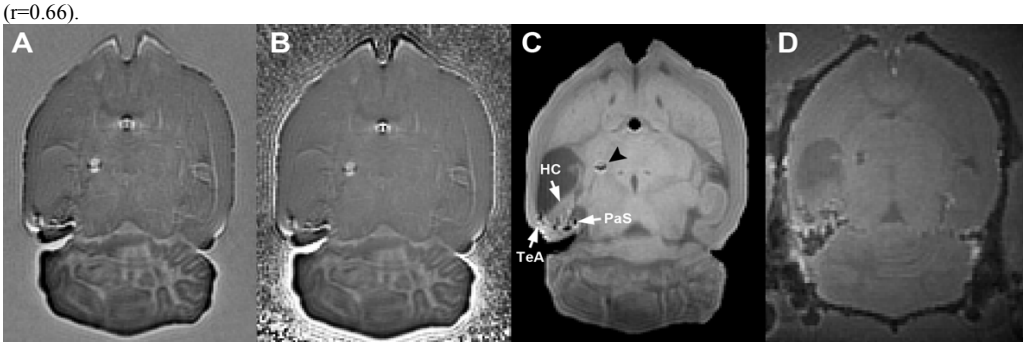

Fig. 1: (**A**) Imaginary, (**B**) phase and (**C**) magnitude SWIFT images of an *ex vivo* rat brain after traumatic brain injury. (**D**) *In vivo* magnitude SWIFT image of the same animal. Black arrowhead points the thalamic calcification. Abbreviations: HC: hippocampus; PaS: parasubiculum; TeA: temporal association cortex.

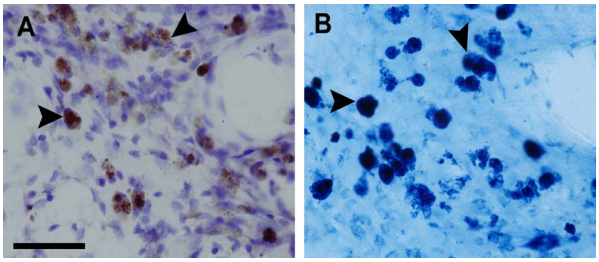

Fig. 2: High magnification photomicrograph of the temporal association cortex (**Fig. 1C**) from Nissl (**A**) and Perl´s (**B**) stained sections. Arrowheads point to high iron content deposits. Scale bar: 50 µm.

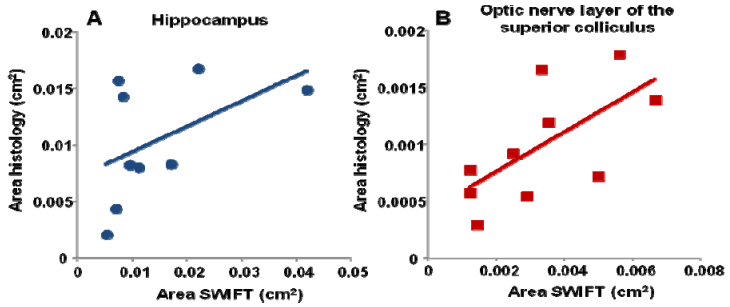

Fig. 3: Correlations of areas of high iron content deposits between SWIFT and histology (cm^2) in the hippocampus (**A**) and the optic layer of the superior colliculus (**B**).

DISCUSSION

Small hemorrhages in brain tissue after traumatic brain injury are detectable by SWIFT without post-processing of the phase images. Iron deposits were identified *in vivo* and *ex vivo* in magnitude and phase components of the SWIFT images, confirmed in the imaginary component image as dipoles, and compared to histology. The signal in SWIFT corresponded closely with regions of high iron content. The magnetic field created by the deposits seemed to be bigger than the actual size in histology, as expected, but complicates direct comparison of image and histology. Further model based analysis and quantification will likely help. The detection of iron deposits and calcifications[3] with SWIFT demonstrates that this technique could be used to detect various aspect of the disease progression after onset of TBI including micro hemorrhages.

REFERENCES

[1]Aronowski and Zhao, Stroke, 2011, [2]Idiyatullin *et al*., JMR, 2006. [3]Lehto *et al*., ISMRM, 2011.

ACKNOWLEDGEMENTS

Academy of Finland, ASLA-Fulbright, Finnish Cultural Foundation, Finnish Foundation for Technology Promotion and grants NIH P41 RR008079, R21 CA129688, and MMF 3932-9227-09.